Analysis, Simulation and Testing of π-type Resonant Link DC-DC Converters[†]

Bill M. Diong
Electrical Engineering
U. of Texas - Pan American
1201 W. University Drive
Edinburg, TX 78539
Ph: (956) 381-2402
Fax: (956) 381-3527

Rene J. Thibodeaux
Electrical Technology Branch
Propulsion Division
Air Force Research Lab

Abstract

High-frequency resonant power converters are well-suited for use in applications requiring high power density converters, as on air and space vehicles (topic 4). However, the properties of many topologies have yet to be thoroughly investigated. This paper presents the results of theoretical analysis, computer simulations and experimental testing performed on one class of (previously uninvestigated) DC-DC resonant converter topologies.

[†] This work was supported in part by the Air Force Office of Scientific Research, Bolling AFB, DC, and Wright Labs, Wright-Patterson AFB, OH.

Analysis, Simulation and Testing of π-type Resonant Link DC-DC Converters

I. INTRODUCTION

High-frequency resonant power converters ([1] and references within) are becoming more widely used as the demand grows for high power density power processors. These converters have been known for some time to be particularly suitable for vehicular applications [2]. More recently, an orderly search of 3-element resonant converter topologies was provided in [3]. Also, reference [4] discussed 3- and 4-element resonant circuit topologies for such converters under voltage/current driven and voltage/current sink options. Furthermore, based on their circuit element connections and source and load excitation types, those topologies were classified into resonant and non-resonant topologies, and on their physical realizability. Many of the topologies 'uncovered' by [3] and classified in [4] have not yet been thoroughly investigated, including those now described below (as evidenced by both a literature search and a patent search).

Figure 1 below shows the block diagram of a typical resonant converter system. The main difference between the system that was studied and other resonant converter systems lies in the resonant circuit portion of the converter. The following section will elaborate on the characteristics of the class of converters studied. The results of computer simulations are also described as are the corresponding experimental results.

II. ANALYSIS OF π-TYPE RESONANT LINK CONVERTERS

Figure 2 below shows a converter topology that will be referred to in the following as the π-type resonant link converter topology, where Z_1, Z_2 and Z_3 are the impedances of the 3 reactive elements (either capacitors or inductors) making up the resonant circuit. It is the effect of this difference in the resonant circuit on the converter's characteristics that was investigated. Among the major properties determined were the converter's voltage transfer function, efficiency, input and output impedances and device stresses.

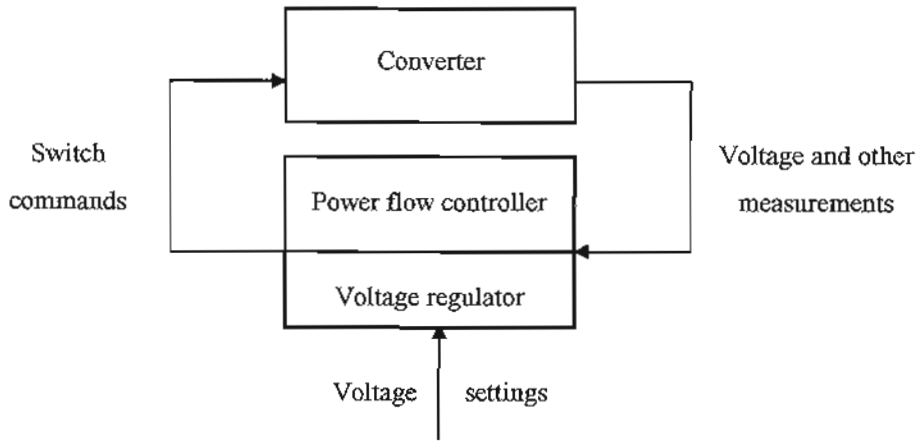

Figure 1 - Block diagram of converter system

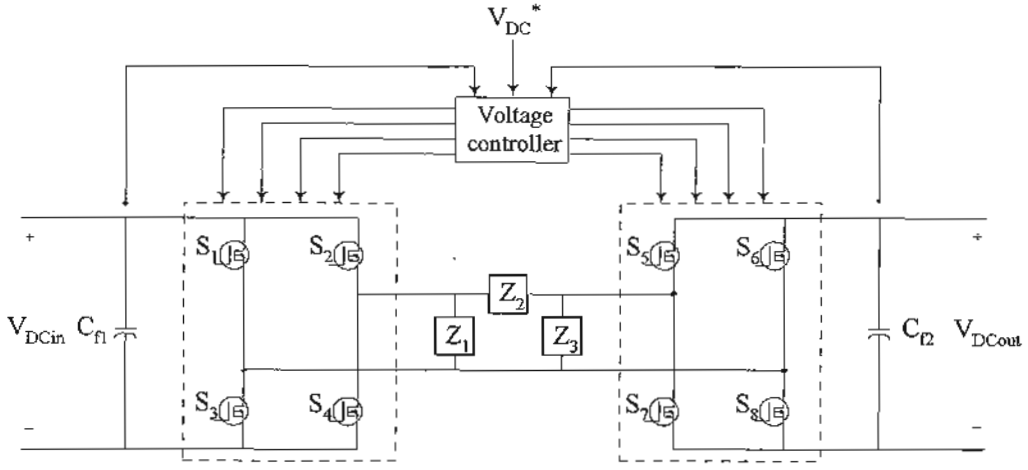

Figure 2 - π-type topology

In this paper, we confine our attention to the case where the resonant circuit is structurally symmetrical, i.e., Z_1 and Z_3 are either both capacitive or both inductive (although they may have different values). Two different possible circuits are analyzed below:

A. The π-type LCL resonant converter

Analysis of this π-type converter, with $Z_1 = L_{out}$, $Z_2 = C$ and $Z_3 = L_{in}$, was based on the assumptions that:

- the transistor and diode {MOSFET} form a resistive switch whose on-resistance is linear with value of R_{ds}, the parasitic capacitances of the switch are neglected, and switching time is zero,
- the elements of the resonant circuit are passive, linear, time-invariant, and do not have parasitic reactive components, and
- loaded quality factor is sufficiently high so that current through the resonant circuit is sinusoidal.

For power flow from left to right, those assumptions yield the following circuit model for the converter with the left-side bridge circuit and resonant circuit behaving as a resonant inverter circuit. The right-side bridge circuit (with all switches off and behaving as a diode rectifier) and resistive load is modeled by an equivalent resistance $R_i = \frac{\pi^2}{8} R_l$ acting as a load to the resonant inverter circuit.

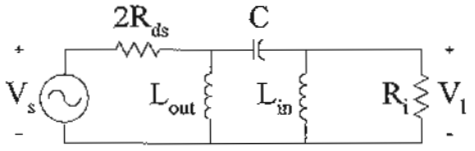

Figure 3 – Model of π-type LCL resonant converter

The input impedance of this equivalent circuit is, in general, given by

$$Z_i(\omega) = \frac{R_i L_{out}(1 - \omega^2 L_{in} C) + j\omega L_{out} L_{in}}{L_{in}(1 - \omega^2 L_{out} C) + j\omega R_i[(L_{out} + L_{in})C - \frac{1}{\omega^2}]} + 2 R_{ds}$$

Suppose $L_{out} = L_{in}$ and $\omega_o := \frac{1}{\sqrt{L_{out} C}}$, then

$$Z_i(\omega) = \frac{R_i L_{out}[1 - (\frac{\omega}{\omega_o})^2] + j\omega {L_{out}}^2}{L_{out}[1 - (\frac{\omega}{\omega_o})^2] + j\omega R_i(\frac{2}{\omega_o^2} - \frac{1}{\omega^2})} + 2 R_{ds}$$

Supposing further that $\omega = n\omega_o$, where n is a positive integer, then

$$Z_{i,n} = \frac{R_i L_{out}(1 - n^2) + jn\omega_o L_{out}^2}{L_{out}(1 - n^2) + j\frac{R_i}{n\omega_o}(2n^2 - 1)} + 2R_{ds}$$

With regard to the currents, voltages and powers in the circuit, first note that $v_s(t)$, generated by the switching of the left-side bridge circuit, is a periodic waveform that looks like the following

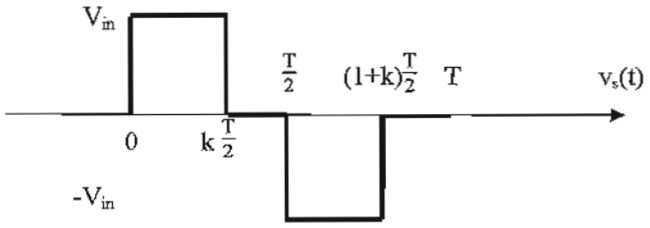

where $k \in [0,1]$ represents the duty-cycle of the switches and T is the period of the equivalent source voltage waveform. Hence the Fourier series representation of $v_s(t)$ is

$$v_s(t) = \sum_{n=1,3,5\ldots}^{\infty} (-1)^{\frac{n-1}{2}} \frac{2V_{in}}{n\pi} \sin\left(\frac{kn\pi}{2}\right) \sin(n\omega_s[t + \frac{1-k}{4}T])$$

with ω_s being the fundamental frequency of $v_s(t)$. Then from the equations for $v_s(t)$ and $Z_{i,n} = Z_i(n\omega_s)$ one can obtain the source current $i_s(t)$ as

$$i_s(t) = \sum_{n=1,3,5\ldots}^{\infty} I_{s,n} \sin(n\omega_s[t + \frac{1-k}{4}T] - \theta_n)$$

where

$$I_{s,n} = \frac{(-1)^{\frac{n-1}{2}} \frac{2V_{in}}{n\pi} \sin\left(\frac{kn\pi}{2}\right) \sin(n\omega_s[t + \frac{1-k}{4}T])}{|Z_{i,n}|}, \qquad \theta_n = \angle Z_{i,n}$$

A conservative upper bound on peak values can be obtained by summing magnitudes of all harmonics.

Concerning the voltage transfer function of this converter, in general, it is given by

$$\frac{V_l}{V_s} = \frac{\frac{1}{j2\omega R_{ds}C}}{(1 - \frac{1}{\omega^2 L_{out}C} - \frac{j}{2\omega R_{ds}C})(1 - \frac{1}{\omega^2 L_m C} - \frac{j}{\omega R_i C}) - 1}$$

Suppose $L_{out} = L_{in}$ and $\omega_o := \frac{1}{\sqrt{L_{out}C}}$, then

$$\frac{V_l}{V_s} = \frac{\frac{1}{j2\omega R_{ds}C}}{[1 - (\frac{\omega_o}{\omega})^2 - \frac{j}{2\omega R_{ds}C}][1 - (\frac{\omega_o}{\omega})^2 - \frac{j}{\omega R_i C}] - 1}$$

Supposing further that $\omega = \omega_o$, then

$$\frac{V_l}{V_s} = \frac{\frac{jR_i}{\omega_o C}}{(\frac{1}{\omega_o C})^2 + 2R_{ds}R_i}$$

For power flow from right to left, all of the above equations are valid, by symmetry, provided the appropriate substitutions are made.

B. The π-type CLC resonant converter

The analysis of this converter, with $Z_1 = C_{out}$, $Z_2 = L$ and $Z_3 = C_{in}$, was based on the same 2 assumptions as for the π-type LCL resonant converter analysis. Those assumptions yield the following circuit model for the converter with the left-side bridge circuit and resonant circuit behaving as a resonant inverter circuit. The right-side bridge circuit (with all switches off and behaving as a diode rectifier) and resistive load is modeled by an equivalent resistance $R_i = \frac{\pi^2}{8} R_l$ acting as a load to the resonant inverter circuit.

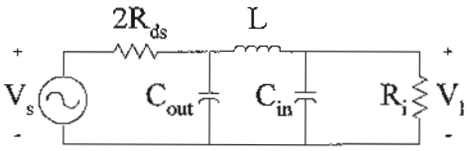

Figure 4 - Model of π-type CLC resonant converter

The input impedance of this equivalent circuit is, in general, given by

$$Z_i(\omega) = \frac{R_i(\omega^2 LC_{in} - 1) - j\omega L}{\omega^2 LC_{out} - 1 + j\omega R_i(\omega^2 LC_{in}C_{out} - C_{in} - C_{out})} + 2R_{ds}$$

Suppose $C_{out} = C_{in}$ and $\omega_o := \frac{1}{\sqrt{LC_{out}}}$, then

$$Z_i = \frac{R_i[(\frac{\omega}{\omega_o})^2 - 1] - j\omega L}{(\frac{\omega}{\omega_o})^2 - 1 + j\omega R_i C_{out}[(\frac{\omega}{\omega_o})^2 - 2]} + 2\,R_{ds}$$

Supposing further that $\omega = n\omega_o$, where n is a positive integer, then

$$Z_{i,n} = \frac{R_i(n^2 - 1) - jn\omega_o L}{n^2 - 1 + jn\omega_o R_i C_{out}(n^2 - 2)} + 2\,R_{ds}$$

With regard to the currents, voltages and powers in the circuit, recall that $v_s(t)$ again has the Fourier series representation given above. Then from the equations for $v_s(t)$ and $Z_{i,n} = Z_i(n\omega_s)$ one can obtain the source current $i_s(t)$ as

$$i_s(t) = \sum_{n=1,3,5\ldots}^{\infty} I_{s,n} \sin(n\omega_s[t + \tfrac{1-k}{4} T] - \theta_n)$$

where

$$I_{s,n} = \frac{(-1)^{\frac{n-1}{2}} \frac{2V_{in}}{n\pi} \sin(\frac{kn\pi}{2}) \sin(n\omega_s[t + \frac{1-k}{4} T])}{|\,Z_{i,n}\,|}, \qquad \theta_n = \angle\, Z_{i,n}$$

A conservative upper bound on peak values can be obtained by summing magnitudes of all harmonics.

Concerning the voltage transfer function of this converter, in general, it is given by

$$\frac{V_l}{V_s} = \frac{\frac{j\omega L}{2R_{ds}}}{(\frac{j\omega L}{2R_{ds}} + 1 - \omega^2 LC_{out})\,(\frac{j\omega L}{R_i} + 1 - \omega^2 LC_{in}) - 1}$$

Suppose $C_{out} = C_{in}$ and $\omega_o := \frac{1}{\sqrt{LC_{out}}}$, then

$$\frac{V_l}{V_s} = \frac{\frac{j\omega L}{2R_{ds}}}{[\frac{j\omega L}{2R_{ds}} + 1 - (\frac{\omega}{\omega_o})^2]\,[\frac{j\omega L}{R_i} + 1 - (\frac{\omega}{\omega_o})^2] - 1}$$

Supposing further that $\omega = \omega_o$, then

$$\frac{V_1}{V_s} = \frac{-j\omega_o L R_i}{(\omega_o L)^2 + 2R_{ds}R_i}$$

For power flow from right to left, all of the above equations are valid, by symmetry, provided the appropriate substitutions are made.

III. COMPUTER SIMULATIONS

Computer simulations were performed using MicroSim PSpice software to verify the analysis and validate the control system design. The simulated output voltage response of the (unregulated) π-type LCL resonant converter, with the following parameters, is shown as Figure 5 below: $V_{DCin} = 270$ V, $C_{f1} = C_{f2} = 20\mu$F, Lout = Lin = 34 μH, C = 0.47 μF, $R_l = 10\ \Omega \Rightarrow R_i = 12.34\ \Omega$, $\omega_s = 80{,}000\pi$ rad/s.

IV. EXPERIMENTAL RESULTS

A hardware implementation of the π-type LCL resonant converter is being constructed. Tests will be performed, specifically, one corresponding to the computer simulation described above to validate that result.

V. CONCLUSIONS

Several novel resonant converter topologies have been analyzed to establish their characteristics. These need to be compared to the characteristics of presently well-known resonant converters to determine their relative advantages and disadvantages.

Simulations of these topologies were performed that validated the analytical results; a typical example was shown. Experiments are being carried out, with the results to be included in the final paper, for verifying both the analysis and the simulations.

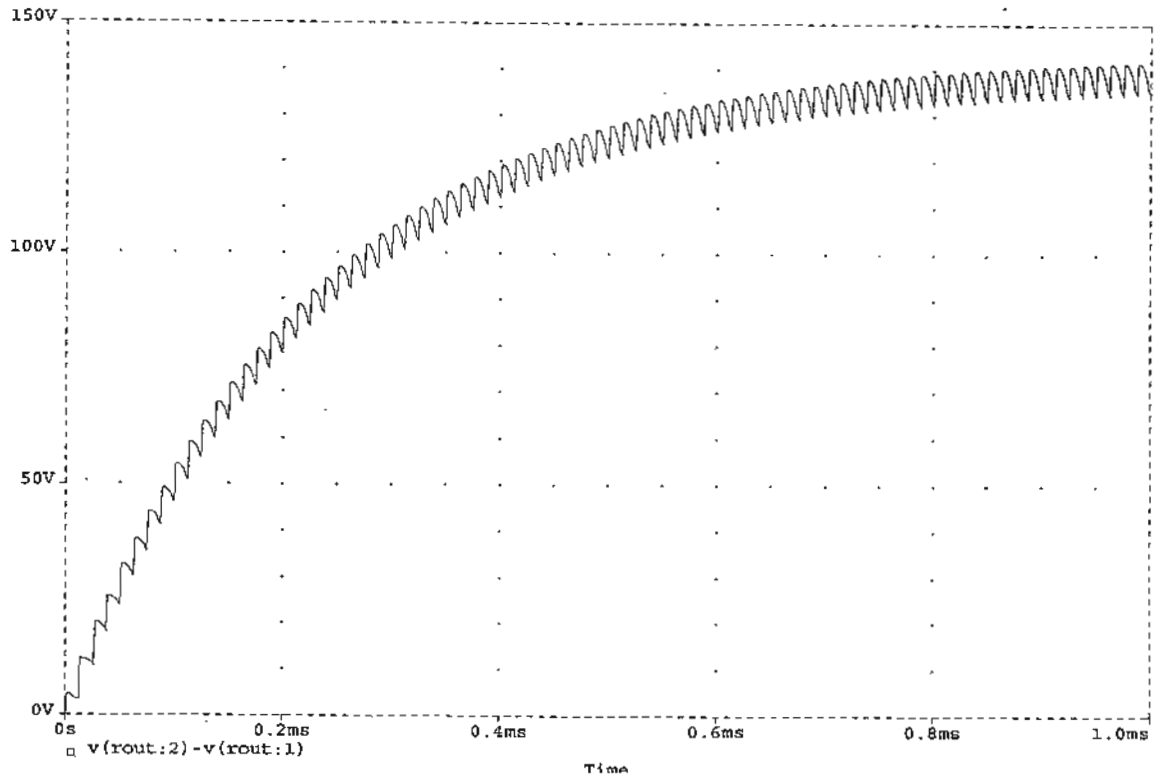

Figure 4 - Typical output voltage response of π-type LCL resonant converter

REFERENCES

[1] M. K. Kazimierczuk and D. Czarkowski, Resonant power converters, John Wiley & Sons, Inc., New York, 1995.

[2] J. D. van Wyk and D. B. Snyman, "High frequency link systems for specialized power control applications," Conf. Rec. IAS Annual Meeting, pp. 793-801, 1982.

[3] R. P. Severns, "Topologies for three-element resonant converters," IEEE Trans. Power Electronics, vol. 7, no. 1, pp. 89-98, Jan 1992.

[4] I. Batarseh, "Resonant converter topologies with three and four energy storage elements," IEEE Trans. Power Electronics, vol. 9, no. 1, pp. 64-73, Jan 1994.